# Three-Dimensional Assemblies of Gold Colloids in Nanoporous Alumina Membranes☆

**Taka-aki Hanaoka[a,b], Hans-Peter Kormann[a], Michael Kröll[a], Thomas Sawitowski[a], and Günter Schmid*[a]**

Institut für Anorganische Chemie, Universität Essen,[a]
Universitätsstrasse 5–7, D-45177 Essen, Germany
Fax: (internat.) + 49 (0)201/183 2402
E-mail: guenter.schmid@uni-essen.de

National Institut of Materials and Chemical Research,[b]
Higashi 1-1, Tsukaba 305, Japan
Fax: (internat.) + 81 (0)298/544487
E-mail: hanaoka@nimc.go.jp

Received December 22, 1997

**Keywords:** Gold colloids / Self-assembly / Nanoporous alumina / Three-dimensional organization

Examples of a new class of three-dimensionally arranged gold colloids have been prepared in the nanoscale pores of alumina membranes. Immobilization of the colloid particles was achieved by a modification of the inner walls with alkoxysilanes $Y–(CH_2)_x–Si(OR)_3$ and $Y–(CH_2)_x–SiR(OR)_2$ bearing suitable functional groups (Y = $NH_2$, SH), followed by anchoring of the colloids by self-assembly onto the modified surface. This procedure gives tight and stable ensembles of colloids on the walls. TEM analyses revealed uniform and random colloidal dispersions on the walls in the form of sub-monolayers without any aggregation. UV/Vis spectra of the filled membranes showed an absorption maximum at ca. 525 nm arising from an excitation of the plasmon resonance of the gold colloids. The dimensions of the pores can be "tuned" and given the diverse range of different colloids available, routes to novel catalysts and sensors can be envisaged.

## Introduction

Over the past decade, a wide variety of approaches have been proposed for the construction of nanostructured materials from nanoparticles. Organization of nanoscale particles is considered as a promising route for the development of new materials that can be classified as nanostructures. Since metal colloids represent one of the most extensively studied classes of nanoscale materials, and because they have the advantage of well-defined size and character, such systems are promising candidates for use as building blocks in the construction of nanostructured materials.[1] Nanostructures constructed from colloids are of interest for a wide range of applications[2] as a result of their chemical, catalytic, electrochemical, magnetic, and optical properties. For example, in catalysis they can be regarded as offering intermediate situations between homogeneous and heterogeneous catalysts[3], and unique catalytic features in reactions such as hydrogenation[4], hydrosilylation[5], and photocatalytic reactions[6] have been reported. Meanwhile, the adsorption of metal colloids onto organic and inorganic supports has been investigated as a means of preparing well-defined heterogeneous catalysts.[7]

Immobilization of metal colloid particles on a suitable structured matrix using a self-assembly technique is one of the most promising strategies for the construction of colloidal nanostructures.[8] Based on such a strategy, the preparation of two-dimensional metal colloid arrays on a flat surface has been reported by Natan et al.[9] and by Sato et al.[10] The use of colloids offers several advantages: (i) essentially monodispersed metal particles are easily obtained, (ii) the preparation and characterization of many kinds of colloidal metals has been well-researched, (iii) ordering of colloids is expected by self-assembly, (iv) anchoring on supports increases stability against agglomeration, and (v) new characteristics originate from an interaction between the colloidal particles and supports.

Since the construction of three-dimensional ensembles is necessary for the practical use of colloids, the development of three-dimensional structures from two-dimensional arrays is necessary.[11] Three-dimensional colloid arrangements have been reported to be produced from multi-layer films by sequential self-assembling[12] and by using sol-gel techniques[13], as well as from the use of reversed micelles[14], and by an external electric field induced layering of colloid crystals.[15] Assembling a homogeneous dispersion in a well-defined three-dimensional nanostructure offers an alternative route to these "stepwise"[12][13][14][15] constructions. Such a strategy requires careful selection of the appropriate matrix. Since a porous alumina membrane, which can be prepared by anodic oxidation of aluminum in diprotic acid solution, has a huge number of parallel pores of uniform diameter, we chose it as a promising matrix for supporting assemblies of colloids. The dimensions of the pores can be controlled by adjusting the anodization con-

  1434–1948/98/0606–0807 $ 17.50+.50/0 

ditions; by varying the applied voltage their diameter can be varied from 5 to 150 nm and their depth, i.e. the thickness of the membrane, from 1 to >100 μm.[16] Such a porous alumina membrane has also been used as a unique template in the assembly of nanostructures.[17] The anodization procedure is readily applicable for the preparation of a membrane of large area and of appropriate shape. Here, we describe the assembly of gold colloids in the well-ordered pores of alumina membranes using a self-assembly technique. These materials belong to a new class of three-dimensional nanostructures, the structures of which can be "tuned" by modification of the matrix. Therefore, this strategy should be a potentially useful technique in the development of diverse applications in optics, as sensors, and as catalysts.

## Results and Discussion

*Immobilized Colloids in Membranes:* Scheme 1 illustrates our strategy for the preparation of the target material and the colloid coordination. The procedure consists of the anodization of aluminum, the derivatization of pores in the alumina membrane with a functionalized alkoxysilane such as $Y-(CH_2)_x-Si(OR)_3$ or $Y-(CH_2)_x-SiR(OR)_2$ (Y = SH, $NH_2$), and the immobilization of colloidal particles.

Scheme 1. Modification of alumina membranes with functionalized alkoxysilane molecules and chemisorption of gold colloids

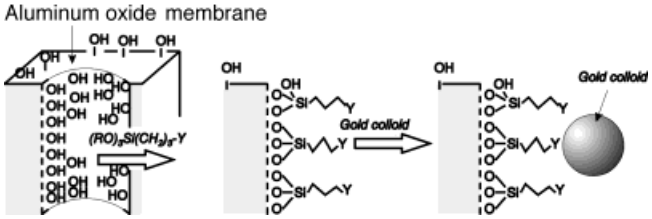


Aluminum plates form porous membranes on the surface upon anodization in 2% phosphoric acid solution. Pore size and pore density is largely governed by the applied voltage.[16] Membranes containing pores of 150 ± 10 nm in diameter are obtained by constant voltage anodization at 150 V. Detachment of the membrane by treatment with sulfuric acid gives a self-standing alumina membrane with a thickness of between 20 and 90 μm depending on the anodization period.

The hydroxyl groups present on the alumina surface are highly reactive and react readily with alkoxysilane molecules generating covalent Al−O−Si moieties. Functional groups Y are selected such that they show good affinity to the metal colloid. Reactions of the alkoxysilanes with the pore walls proceed smoothly in toluene solution under reflux conditions. The IR spectrum of a membrane reacted with 3-aminopropylmethyldiethoxosilane (APDMS) shows two signals at 2960 and 2930 $cm^{-1}$, which can be attributed to C−H stretching vibrations of the alkyl chains.[18] By monitoring the peak intensity during the course of the reaction, saturation is observed after ca. 14 h. The reactivity of the reagents is modified by the nature of the functional group Y and by the number of alkoxy groups. Compared to dialkoxysilanes, trialkoxysilanes show lower reactivity. On the other hand, aminoalkoxysilanes are highly reactive compared to mercapto derivatives.

The immobilization of gold colloids in the pores can be performed by one of two types of vacuum incorporation. In the first, the modified membrane is placed on a short plastic tube connected to a water pump, and the gold colloid solution is sucked through the membrane. Alternatively, the membrane is placed in a flask and the colloid solution is added. Evacuation of the flask causes the solution to penetrate into the pores. In both cases it is necessary to exhaustively wash out remaining silane before the filling process. Even small amounts of unreacted reagents cause immediate aggregation of the gold colloids. Well-washed membranes take on a dark-red color upon incorporation of gold colloids. Figure 1 shows a schematic depiction of a membrane containing immobilized gold.

Figure 1. Model structure of a colloid-charged porous alumina membrane

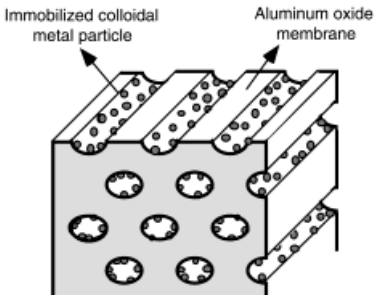


*Optical Properties:* UV/Vis spectra of gold colloid solutions, prepared as described[21], show an absorption maximum at ca. 520 nm originating from an excitation of plasmon resonance.

Figure 2. UV/Vis spectra of immobilized gold colloids in nanoporous membranes derivatized with different alkoxysilanes − A: derivatized with APDMS; B: derivatized with MPDMS

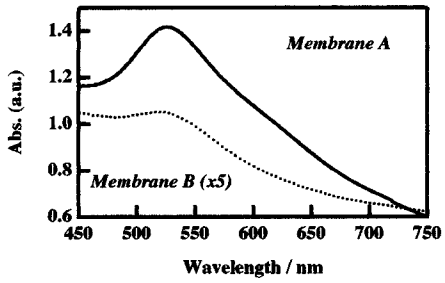


The spectra of colloids in membranes show resonances at approximately the same position. Figure 2 shows the spectra of two colloid-containing membranes. Membrane A was modified with APDMS, membrane B with 3-mercaptopropylmethyldimethoxysilane (MPDMS). Both spectra show a peak at $\lambda_{max}$ = ca. 525 nm, but the relative ab-

sorbances differ markedly. The peak position is close to that of the original solution, albeit slightly shifted to longer wavelengths. This shift can be explained in terms of interparticle coupling between the colloids[19], i.e. a reduction of the distance between particles compared to that in solution.

The difference in the absorbances of membranes A and B can be attributed to the different amounts of colloid that are immobilized. The different degree of immobilization can be explained by preferred interactions between the amino functions of APDMS and the colloids bearing citric acid molecules on the surface. The SH functions in MPDMS could be expected to form strong bonds to gold particles, but this effect is less in evidence compared to the acid-base interaction. Since neither spectrum shows aggregation peaks between 600 and 800 nm, aggregation of the colloids by migration can be excluded. The lack of aggregation indicates that the colloids are tightly bound to the surface through their interaction with the functional groups of anchored molecules. Assuming that the pores have a diameter of 160 nm and that there is a pore density of $1.1 \cdot 10^9$ $cm^{-2}$, in accordance with the data of Rigby and co-workers[16c], the internal surface area of the pores can be roughly calculated as $4 \cdot 10^2$ $cm^2$ for 1 $cm^2$ of membrane. The outer surface area is thus less than 1% of this value. Since the density of surface hydroxy groups on the alumina was reported to be 10 per $nm^2$ after treatment at 100°C[20], the total number of OH groups in the pores can be estimated as $4 \cdot 10^{16}$ for 1 $cm^2$ of membrane. If all OH groups are derivatized by silane molecules, about 23 nmol of functional groups are fixed in the pores. Considering the size of the colloid (13 nm), more than ca. 450 of the functional groups can be expected to be present within the area corresponding to the dimensions of one colloid particle. Of course, not all functional groups are able to interact with the colloids, but strong interactions by multi-anchoring between the surface and the particle are very reasonable as an interpretation of the absence of aggregation.[22]

*Transmission Electron Microscopy:* To confirm the dispersion of the colloids on the derivatized surface of the pores, transmission electron microscopy (TEM) investigations were carried out on sectioned samples. Figure 3 shows a TEM image of a porous membrane following derivatization with APDMS and treatment with a gold colloid by vacuum incorporation.

The gold colloid particles can clearly be recognized on the pore walls. Apart from the region near the surface of the membrane, the particles are randomly and uniformly distributed and cover the wall surface as a sub-monolayer extending over a large area. No aggregated or chained particles can be observed in either direction, i.e. in the plane of, or perpendicular to the wall. In contrast, a TEM image of an underivatized porous membrane following treatment with the colloid revealed only the presence of partly aggregated colloids of low density. Therefore, the random arrangement indicated by the UV/Vis spectrum is clearly confirmed by the TEM observation.

The average diameter of the immobilized colloids on the wall is found to be ca. 15 nm (for 131 measured particles).

Figure 3. TEM image of immobilized gold colloids (ca. 13 nm) in opened pores of alumina

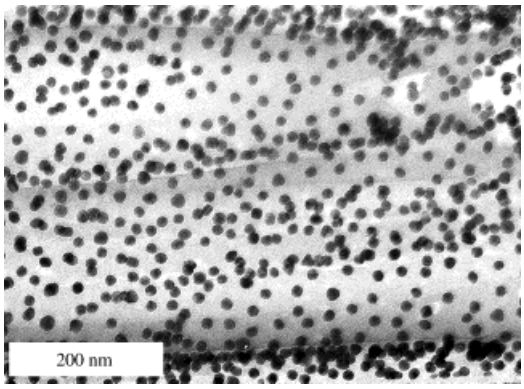


This value is slightly larger but close to the size of the original colloids in aqueous solution, i.e. the colloidal particles do not grow or aggregate during immobilization. The sub-monolayer coverage of the wall with the gold colloids was found to represent ca. 25% of a full monolayer. Incomplete coverage of the wall can be attributed to an electrostatic repulsion between particles. This is consistent with previous observations on a two-dimensional array of gold colloids on a derivatized $SiO_2$ surface.[9]

Since the pores are cylindrical in shape, the walls are concave. Therefore, the particle density projected on the film appears to vary with position in the pore. Differently sectioned TEM photographs clearly show the effect of pore shape. Figures 4a to 6a show images of apparently different dispersions according to the sectioning, along with schematic depictions.

In order to make TEM imaging easy, Anopore™ with 250 nm pore widths was used for this special purpose. The sample was derivatized with APDMS and sectioned into sheets of thickness 100 nm. A part of the sample gave images showing the particles located only near the pore walls (Figure 4a). In this micrograph, closely packed, vertically overlapped particles are observed along the walls. This arrangement is interpreted as illustrated in Figure 4b. In this image, thin sectioning is considered to remove both walls, i.e. the upper and lower faces, of the pore. Since particles near the wall are viewed from the perpendicular direction, particles aligned vertically give a projected image of overlapped particles. As the result, the density of particles near the wall appears to increase. Figure 5a shows an image of an area similar to that depicted in Figure 4a (bottom), but additionally shows a pore with an intact rear side (upper part). Figure 5b illustrates a tubular pore cut in half, with immobilized particles on the surface. In accordance with the curvature of the bottom side, the apparent density of particles appears to be higher near the vertical walls and gradually decreases towards the center.

Figure 6a depicts two distinct areas in one pore (parts A and B). The two areas are distinguishable by the following criteria: (i) the observed density of particles in part A is much higher than that in part B, (ii) overlapped images of particles are apparent only in part A, (iii) the darkness

Figure 4. (a) TEM image of gold colloids in the pores. Both the upper and lower walls have been removed by sectioning; (b) schematic representation illustrating the situation

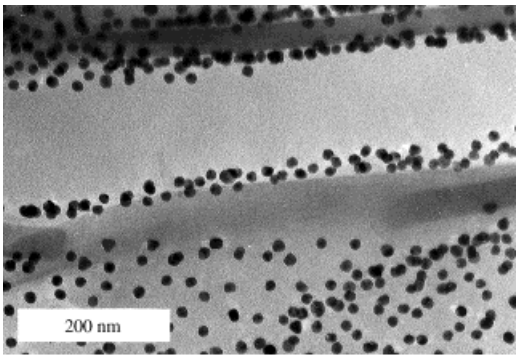


a

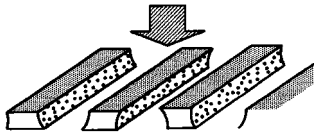

b

Figure 5. (a) TEM image of gold colloids in alumina pores opened on one side, (b) schematic representation to clarify the photograph

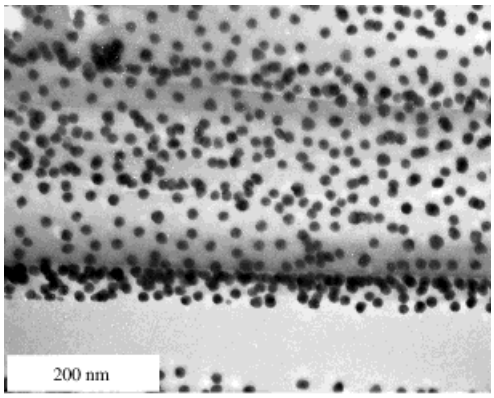


a

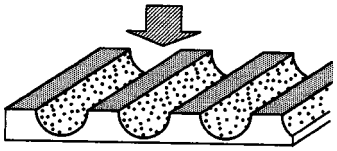

b

Figure 6. (a) Some distinct areas in a piece of membrane supporting gold colloids. Area B shows part of a pore opened on one side, while area A depicts a view through a thin, but colloid-bearing alumina wall; the density of colloids appears higher in A than in B due to the simultaneous imaging of particles on both the front and rear sides. The schematic representation in Figure 6b helps to clarify the relatively complicated situation in Figure 6a.

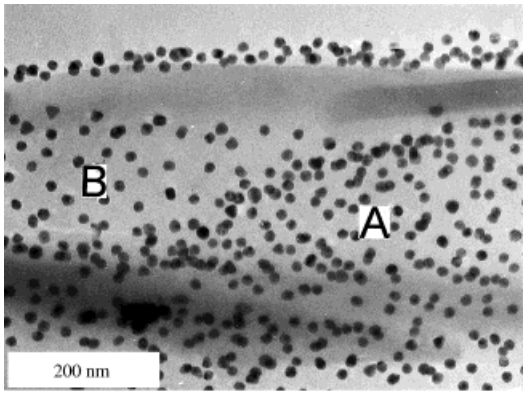


a

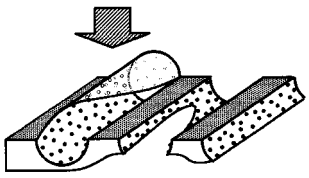

b

around the colloids in area A is more pronounced than that in area B. Part B is considered to be similar to the bottom part of a wall, as in Figure 4b. Figure 6b illustrates a cylindrical pore sliced slantwise. This scheme depicts two parts; one part is modelled in Figure 5b, while the other consists of a whole pore wall. The image of area A is assigned to a transmission view of the whole tube, i.e. the overlapped image of both upper and lower walls of one pore. This view can be considered to give an almost double particle density and an overlapped image of particles through projection of both walls within the same area. The model shown in Figure 6b interprets all characteristics of Figure 6a.

These three TEM photographs are consistent with the results of spectroscopic studies and clearly confirm the situation with gold colloids immobilized on the tubular walls of alumina membranes.

### Conclusions

Gold colloids have been successfully immobilized in the parallel and uniform pores of alumina membranes. The ensemble of colloids forms a sub-monolayer on the pore walls (coverage = ca. 0.25), as shown by TEM and UV/Vis spectroscopy. The observations show that the colloids are tightly anchored on the surface, randomly and uniformly, without any aggregation. Thus, three-dimensionally arranged colloidal particles are distributed over a large area, as a result of their self-assembly on the derivatized surfaces of the structurally well-defined alumina. The thickness of the membranes in which the colloids are arranged ranges from 10 to 100 μm, and the pore size can be "tuned" by variation of the anodization conditions. Variation of the anchored colloids should be easily achieved by means of suitable combinations of derivatizing reagents and colloidal metals.

## Experimental Section

*General:* Aluminum plates of 99.5% of purity were used. Of the alkoxysilanes used as derivatizing reagents, 3-mercaptopropylmethyldimethoxysilane (MPDMS) was purchased from ABCR GmbH & Co., Germany, while 3-aminopropylmethyldiethoxysilane (APDMS) was purchased from Fluka GmbH, Switzerland. Toluene was obtained as analytical grade and was dried by distillation from sodium benzophenone ketyl. Analytical grade methanol was used without further purification. Gold colloid solutions were prepared by an established method[21] through reduction of $HAuCl_4$ with sodium citrate. The average diameter of the colloids was measured as 13 ± 1 nm. Commercially available porous aluminum oxide membrane, Anopore™ (Merck, Germany; average pore diameter 250 nm), was also used as a porous alumina membrane.

*Physical Measurements:* IR spectra of derivatized membranes were recorded on a BIO-RAD FTS-175 infrared spectrometer. Electronic spectra of membranes containing gold colloids were measured on a Varian Cary-1 UV/Vis spectrometer equipped with a small aperture fitted to the sample. TEM images were obtained using a Philips CM 200 FEG microscope. Samples for TEM were embedded in a resin and sectioned. The thickness of the sample was varied from 100 to 50 nm. An Ultra Cut Microtom, Leica, Germany, was used for sectioning.

*Preparation of Porous Alumina Membranes:* Aluminum plates (99.5%, 70 × 55 × 2 mm) were electropolished before anodization in a mixture of sulfuric acid and phosphoric acid. Anodic oxidation was carried out in 2% (w/w) phosphoric acid under a constant voltage of 150 V at 6°C. The maximum current density was ca. 2.5 mA $cm^{-2}$. Anodization was allowed to proceed for 6 to 48 h depending on the required thickness of the membrane. Thereafter, the applied voltage was reduced in a stepwise manner from 150 V to 0.5 V and then stopped. The anodized plates were washed with water and dried in air, then immersed in 12.5% sulfuric acid at room temperature in order to detach the porous alumina membranes. The membranes were carefully washed with water and then immersed in 10% sulfuric acid for 10 min to remove the barrier layer on the rear side, so as make through pores. Subsequently, the membrane was rinsed with water and methanol, and dried.

*Derivatization of Porous Alumina:* A typical procedure for the derivatization with MPDMS and APDMA was as follows: the membrane was cut to a size of ca. 1 × 2 cm, then washed with methanol, and dried in air. Subsequent procedures were carried out under nitrogen. The specimen was placed in a 50 ml flask under anhydrous conditions. A dry toluene solution of the derivatization reagent (5%) was added to the flask, heated to reflux temperature, and maintained under these conditions for 18 h without stirring. After cooling, the solution was removed and the membrane was thoroughly rinsed with dry toluene. In order to ensure complete reaction of the surface hydroxy groups with the alkoxysilanes, each specimen was subsequently subjected to the reaction conditions for a further 1 h. Afterwards, the sample was repeatedly washed with hot toluene to ensure complete removal of the unreacted reagent.

*Immobilization:* The implantation of gold colloids into the modified pores was carried out by one of two vacuum filling methods. (a) The membrane was washed with water and then placed on a short plastic tube (⊘ = 5 mm) connected to a water pump via a 3-way control valve. A drop of gold colloid solution was applied to the other side of the membrane and drawn into the pores by applying a vacuum. (b) The washed membrane was placed in a 50-ml round-bottomed flask and 10 ml of the gold colloid solution was added. The flask was then carefully evacuated to water-pump pressure and maintained under these conditions overnight. In both methods, immobilization of the colloids was checked by observing the color of the membrane. After incorporation, the membrane was washed thoroughly with distilled water and dried in air at room temperature.

---

☆ Dedicated to Professor *Hartmut Bärnighausen* on the occasion of his 65th birthday.


[1] [1a] *Clusters and Colloids* (Ed.: G. Schmid), VCH, Weinheim, **1994**, chapter 1. – [1b] G. Schmid, *Chem. Rev.* **1992**, *92*, 1709–1727. – [1c] G. Schön, U. Simon, *Colloid Polym. Sci.* **1995**, *273*, 101–117. – [1d] J. H. Fendler, F. C. Meldrum, *Adv. Mater.* **1995**, *7*, 607–632; M. Giersig, P. Mulvaney, *J. Phys. Chem.* **1997**, *97*, 6334–6336. – [1e] R. G. Freeman, K. C. Grabar, K. J. Allison, R. M. Bright, J. A. Davis, A. P. Guthrie, M. B. Hommer, M. A. Jackson, P. C. Smith, D. G. Walter, M. J. Natan, *Science* **1995**, *267*, 1629–1632.

[2] *Nanomaterials: Synthesis, Properties, and Application* (Eds.: A. S. Edelstein, R. C. Cammarata), Institute of Physical Publishing, Bristol, **1996**, p. 111–140.

[3] D. R. Anton, R. H. Crabtree, *Organometallics* **1983**, *2*, 855–859.

[4] [4] H. Hirai, H. Chawanya, N. Toshima, *Macromol. Chem., Rapid Commun.* **1981**, *2*, 99–103. – [4b] N. Toshima, T. Takahashi, *Bull. Chem. Soc. Jpn.* **1992**, *65*, 400–409. – [4c] H. Bönnemann, W. Brijoux, R. Brinkmann, E. Dinjus, R. Fretzen, T. Joussen, B. Korall, *J. Mol. Cat.* **1992**, *74*, 323–333. – [4d] M. Brust, J. Fink, D. Bethell, D. J. Schiffrin, C. Kiely, *J. Chem. Soc., Chem. Commun.* **1995**, 1655–1656.

[5] [5a] L. N. Lewis, N. Lewis, *J. Am. Chem. Soc.* **1986**, *108*, 7228–7231. – [5b] L. N. Lewis, R. J. Uriarte, N. Lewis, *J. Mol. Catal.* **1991**, *66*, 105–113.

[6] [6a] A. Harriman, *J. Chem. Soc., Faraday Trans.* **1986**, *82*, 2267–2274. – [6b] C. K. Grätzel, M. Grätzel, *J. Am. Chem. Soc.* **1979**, *101*, 7741–7743. – [6c] G. S. Nahor, L. C. T. Shoute, P. Neta, A. Harriman, *J. Chem. Soc., Faraday Trans.* **1990**, *86*, 3927–3933. – [6d] T. Hanaoka, H. Arakawa, K. Takeuchi, T. Matsuzaki, Y. Sugi, *Chem. Express* **1989**, *4*, 137–140. – [6e] T. Hanaoka, Y. Kubota, K. Takeuchi, T. Matsuzaki, Y. Sugi, *J. Mol. Catal. A - Chemical* **1995**, *98*, 157–160.

[7] [7a] G. Schmid, M. Harms, J.-O. Malm, J.-O. Bovin, J. van Ruitenbeck, H. W. Zandbergen, W. T. Fu, *J. Am. Chem. Soc.* **1993**, *115*, 2046–2048. – [7b] K. J. Klabunde, Y.-X. Li, B.-J. Tan, *Chem. Matter.* **1991**, *3*, 30–39.

[8] [8a] A. Badia, S. Singh, L. Demers, L. Cuccia, G. R. Brown, R. B. Lennox, *Chem. Eur. J.* **1996**, *2*, 359–363. – [8b] A. Ulman, *Chem. Review* **1996**, *96*, 1533–1554.

[9] [9a] K. C. Grabar, K. J. Allison, B. E. Baker, R. M. Bright, K. R. Brown, R. G. Freeman, A. P. Fox, C. D. Keating, M. D. Musick, M. J. Natan, *Langmuir* **1996**, *12*, 2353−2361. − [9b] K. C. Grabar, R. G. Freeman, M. B. Hommer, M. J. Natan, *Anal. Chem*. **1995**, *67*, 735−743. − [9c] K. C. Grabar, P. C. Smith, M. D. Musick, J. A. Davis, D. G. Walter, M. A. Jackson, A. P. Guthrie, M. J. Natan, *J. Am. Chem. Soc*. **1996**, *118*, 1148−1153.
[10] [10a] T. Sato, D. Brown, B. F. G. Johnson, *J. Chem. Soc., Chem. Commun*. **1997**, 1007−1008. − [10b] T. Sato, D. G. Hasko, H. Ahmed, *J. Vac. Sci. Technol. B* **1997**, *15*, 45−48.
[11] D. L. Feldheim, K. C. Grabar, M. J. Natan, T. E. Mallouk, *J. Am. Chem. Soc*. **1996**, *118*, 7640−7641.
[12] J. Schmitt, G. Decher, W. J. Dressick, S. L. Brandow, R. E. Geer, R. Shashidhar, J. M. Calvert, *Adv. Mater*. **1997**, *9*, 61−65.
[13] H. Fan, Y. Zhou, G. P. Lopez, *Adv. Mater*. **1997**, *9*, 728−731.
[14] L. Motte, F. Billoudet, E. Lacaze, M.-P. Pilenti, *Adv. Mater*. **1996**, *8*, 1018−1020.
[15] M. Trau, D. A. Saville, A. Aksay, *Science*, **1996**, *272*, 706−709.
[16] [16a] J. P. O′Sullivan, G. C. Wood, *Proc. Roy. Soc. Lond. A* **1970**, *317*, 511−543. − [16b] J. W. Diggle, T. C. Downie, C. W. Goulding, *Chem. Rev*. **1969**, *69*, 365−405. − [16c] R. C. Furneaux, W. R. Rigby, A. P. Davidson, *Nature* **1989**, *337*, 147−149.
[17] [17a] H. Masuda, K. Fukuda, *Science* **1995**, *268*, 1466−1468. − [17b] H. Masuda, M. Satoh, *Jpn. J. Appl. Phys*. **1996**, *35*, 126−129. − [17c] P. Hoyer, N. Baba, H. Masuda, *Appl. Phys. Lett*. **1995**, *66*, 2700−2702. − [17d] C. A. Huber, T. E. Huber, M. Sadoqi, J. A. Lubin, S. Manalis, C. B. Prater, *Science* **1994**, *263*, 800−802. − [17e] J. C. Hulteen, C. R. Martin, *J. Mater. Chem*. **1997**, *7*, 1075−1087.
[18] D. E. Weisshaar, B. D. Lamp, M. D. Porter, *J. Am. Chem. Soc*. **1992**, *114*, 5860−5862.
[19] G. L. Hornyak, C. J. Patrissi, C. R. Martin, *J. Phys. Chem*. **1997**, *101*, 1548−1555.
[20] Y. Iwasawa, *Hyoumen*, **1981**, *19*, 161.
[21] [21a] J. Turkevich, P. C. Stevenson, J. Hillier, *Disc. Faraday Soc*. **1951**, *11*, 55−75. − [21b] G. Schmid, A. Lehnert, U. Kreibig, Z. Adamczyk, P. Belouscheck, *Z. Naturforsch*. **1990**, *45b*, 989−994.
[22] G. Schmid, St. Peschel, Th. Sawitowski, *Z. Anorg. Allg. Chem*. **1997**, *623*, 719−723.

[97315]